

See discussions, stats, and author profiles for this publication at: <https://www.researchgate.net/publication/390402739>

Deep Learning for Early Earthquake Detection: Application of Convolutional Neural Networks for P-Wave Detection

Article in *Applied Sciences* · April 2025

DOI: 10.3390/app15073864

CITATIONS

4

8 authors, including:



[Alisher Skabylov](#)

Al-Farabi Kazakh National University

14 PUBLICATIONS 28 CITATIONS

[SEE PROFILE](#)

READS

121



[Margulan Ibraimov](#)





Al-Farabi Kazakh National University

41 PUBLICATIONS 157 CITATIONS

[SEE PROFILE](#)

Article

Deep Learning for Early Earthquake Detection: Application of Convolutional Neural Networks for P-Wave Detection

Dauren Zhexebay ¹, Alisher Skabylov ¹, Margulan Ibraimov ¹, Serik Khokhlov ¹, Aldiyar Agishev ^{1,2,*},
Gulnur Kudaibergenova ¹, Aibala Orazakova ¹ and Almansur Agishev ¹

¹ Faculty of Physics and Technology, Al-Farabi Kazakh National University, 71/23 Al-Farabi Ave., Almaty 050040, Kazakhstan; zhexebay92@gmail.com (D.Z.); alisher.skabylov@kaznu.edu.kz (A.S.); margulan.ibraimov@kaznu.edu.kz (M.I.); skhokh88@gmail.com (S.K.); moikomp1894@gmail.com (G.K.); aibala.orazakova@gmail.com (A.O.); almansur97@gmail.com (A.A.)

² Data Science in Astrophysics Research Center, Almaty 050040, Kazakhstan

* Correspondence: aldiyar.agishev@gmail.com

Featured Application: Earthquake Detection, Earthquake Early Warning System (EWS), Processing of Seismic data.

Abstract: Early detection of earthquakes is essential for minimizing potential damage and ensuring public safety. Recent advancements in deep learning, particularly convolutional neural networks (CNNs), provide a promising alternative for analyzing seismic waves. In contrast, traditional methods such as the short-term average/long-term average (STA/LTA) algorithm and the Akaike information criterion (AIC) have limitations in detecting primary (P) waves in high-noise conditions, caused by industrial and anthropogenic disturbances. This study presents a CNN-based automatic P-wave detection model tailored for the Almaty city region. The seismic dataset used in this research was obtained from the IRIS database and includes data collected from seven stations within a 333 km radius of Almaty, Kazakhstan. The proposed model achieves a recall rate of 89.1% and an accuracy of 94.1% compared to other deep learning-based models. Experimental results demonstrate that this method enhances the reliability of automatic early earthquake warning systems and improves the accuracy of P-wave detection. The research outputs presented for the local region are unique. Applying CNNs in seismic monitoring facilitates the development of efficient automated systems that minimize risks and improve response measures for natural disasters.

Keywords: P-wave detection; deep learning; convolutional neural networks; earthquake early warning; seismic monitoring



Academic Editor: Nicholas Vassiliou Sarlis

Received: 3 March 2025

Revised: 20 March 2025

Accepted: 26 March 2025

Published: 1 April 2025

Citation: Zhexebay, D.; Skabylov, A.; Ibraimov, M.; Khokhlov, S.; Agishev, A.; Kudaibergenova, G.; Orazakova, A.; Agishev, A. Deep Learning for Early Earthquake Detection: Application of Convolutional Neural Networks for P-Wave Detection. *Appl. Sci.* **2025**, *15*, 3864. <https://doi.org/10.3390/app15073864>

Copyright: © 2025 by the authors. Licensee MDPI, Basel, Switzerland. This article is an open access article distributed under the terms and conditions of the Creative Commons Attribution (CC BY) license (<https://creativecommons.org/licenses/by/4.0/>).

1. Introduction

Natural phenomena such as earthquakes significantly threaten populations, infrastructure, and ecosystems. Although such events cannot be prevented, various strategies can be implemented to mitigate their impact. These include the deployment of early warning seismic stations and advanced data analysis technologies [1]. In this context, early warning systems (EWSs) have become increasingly relevant to minimize damage and ensure public safety [2].

One of the critical components of such systems is the detection of primary (P) waves, which are the first seismic waves to reach the Earth's surface following an earthquake.

Although P waves are less destructive than subsequent secondary (S) waves, their identification is crucial for early warning applications. Detecting P waves enables the prediction of incoming, more dangerous seismic waves, facilitating the timely initiation of evacuation procedures and other protective measures, thus reducing the potential for casualties and structural damage [3].

Accurately determining the timing and location of a seismic wave epicenter is a fundamental aspect of research in this field. One of the significant challenges in seismic wave detection is the low amplitude of ground motion combined with a high noise level. Traditional methods for identifying seismic waves require automation to improve efficiency and reliability. Advancements in high-speed technologies have enabled the collection of seismic data at an unprecedented rate. However, processing such data requires highly efficient analytical methods that minimize errors while maintaining precision. To address these challenges, the field of seismology demands the development of robust and precise automated techniques capable of enhancing the efficiency of data processing and improving the reliability of seismic event detection.

One of the classic methods for the detection and identification of seismic waves is the short-term average/long-term average (STA/LTA) algorithm [4]. However, STA/LTA has inherent limitations; improper selection of initial parameters can lead to inaccurate results. Additionally, under noisy conditions, this algorithm may generate false detections of seismic waves or fail to identify them altogether. Another widely referenced approach for P-wave detection is the Akaike information criterion (AIC) [5]. Despite its utility, this method also has significant drawbacks. One of its main limitations is the inaccurate estimation of the global minimum in the presence of high noise levels, which reduces its reliability in real-world applications. Long-term memory (LSTM) networks are introduced to model the differences between P waves and background noise. Furthermore, the front end of the network often incorporates a short-time Fourier transform (STFT) to preserve implicit information while reducing computational load. However, studies indicate that the accuracy of deep neural networks using the LSTM-STFT approach declines when the amplitude of the P-wave is low and background noise levels are high [6].

Early studies in seismology focused primarily on classical methods for determining the location and magnitude of the earthquake. For instance, in [7], fundamental principles of seismic wave registration and processing were examined to facilitate the estimation of earthquake parameters. In [8], algorithms for automatically detecting P and S waves were proposed, significantly improving the accuracy of time-based measurements. Similarly, in [9], a methodology was developed to analyze the time delays between P and S waves was developed to enhance the accuracy of epicenter localization. These advancements laid the foundation for modern seismic monitoring techniques, paving the way for further improvements by integrating deep learning-based approaches.

The analysis and development of P-wave detection algorithms are crucial research areas in earthquake early warning systems (EEWSs). In their review study, Chandrakumar et al. (2023) [10] evaluated existing P-wave detection methods and algorithms for estimating earthquake magnitude, identifying three main categories: source-based algorithms, wavefield-based algorithms, and local measurement-based algorithms. They also highlighted the increasing interest in recent years in using deep learning methods to enhance P-wave detection accuracy and minimize false alarm rates.

With the advancement of machine learning, neural network models and classification algorithms have increasingly been applied in seismology. As a result, numerous studies have explored using artificial neural networks (ANNs) for seismic data analysis. For example, ref. [11] investigated the potential of ANNs for classifying dynamic features, demonstrating their applicability to seismic data processing. In [12], the application of

convolutional neural networks (CNNs) to identify seismic waves and filter out noise was demonstrated. Ref. [8] highlighted the importance of integrating machine learning methods to enhance prediction accuracy and seismic risk assessment. It is essential to note that the successful application of ANNs in this field requires theoretical advancements and practical implementation. It includes the development of specialized software solutions and hardware systems for real-time seismic activity monitoring [12]. The expansion of machine learning techniques has led to the introduction of various approaches, such as the threshold processing algorithm [13], supervised learning based on classified signals from microseismic monitoring systems [14], the K-means clustering algorithm [15,16], support vector machines (SVMs) [17], wavelet transformation [18], and template matching [19]. However, traditional machine learning methods often require manual feature selection, which can be labor-intensive and not always efficient [20]. These limitations highlight the need for automated feature extraction and deep learning-based approaches to improve seismic event detection and classification.

Modern machine learning technologies and intense learning are opening new frontiers in P-wave detection and are developing effective early warning systems. Artificial neural networks can process large volumes of data and identify complex patterns that may not be apparent through traditional analytical methods. For example, recurrent neural networks (RNNs) enable the modeling of temporal dependencies within seismic data, which is particularly crucial given that the temporal characteristics of seismic signals play a key role in accurate detection [21]. ANN-based systems have the potential to significantly improve both the accuracy and speed of P-wave detection, thus improving the overall efficiency of early warning systems [3].

One of the modern methods for seismic wave detection is the capsule neural network, which demonstrates high accuracy and low false alarm rates. However, its primary drawbacks include relatively slow training and testing speeds, which limits its practical applicability to real-time seismic monitoring systems [22]. In 2019, the PhaseNet neural network model was introduced to detect P waves and S waves. PhaseNet utilizes three-component seismic waveforms as input data and generates probability distributions for P-wave arrivals, S-wave arrivals, and noise as output data [23].

Deep learning models, such as recurrent neural networks, utilize multiple hidden layers to automatically extract meaningful features from raw data, enabling them to process complex time series [24] effectively. This capability makes deep models particularly suitable for seismic data analysis, where it is essential to capture all relevant information contained in waveform patterns [25]. Furthermore, ref. [26] presented a machine learning model based on historical earthquake data for aftershock prediction, contributing to improved seismic risk assessment. Another CNN-based approach for real-time P-wave detection in earthquake early warning systems is Dpick. This method is trained on synthetically generated waveforms that simulate real P waves, allowing it to estimate P-wave arrival times [27] accurately. One of the key advantages of Dpick is its ability to achieve high detection performance without requiring large amounts of training data, making it a practical solution for real-time seismic monitoring. Deep learning has demonstrated significant potential in the field of earthquake prediction. Models such as convolutional neural networks have proven to be highly effective in various tasks, including signal processing [28]. These models can automatically extract critical features from the data, making them particularly useful for analyzing seismic signals [29].

Research on local and regional seismic activity is crucial in understanding earthquake dynamics and improving detection accuracy. In [30], an analysis of seismic events in Southern California using data from the Southern California Earthquake Data Center (SCEDC) identified patterns in magnitude distribution and earthquake frequency. These findings

contribute to a better understanding of regional seismic behavior and its implications for assessing earthquake hazards. In [31], calibration methods for seismic stations were presented to enhance the accuracy of amplitude measurements, which is essential to determine the magnitude of the earthquake. In [3], convolutional neural networks were also trained to estimate the magnitude and frequency of the earthquake directly from seismograms, eliminating manual feature extraction. Furthermore, a CNN-based model was applied to determine the arrival times of the P-wave and the polarity of the first motion using 19.4 million seismograms. This model selected the arrival time in 0.028 s from the picks of the human analyst in 75% of the cases, while the first motion polarity classification reached an accuracy of 95%.

The use of neural networks for P-wave detection and the development of earthquake early warning systems represent promising research directions. These approaches improve the accuracy and speed of seismic event detection and open new possibilities for integrating advanced technologies into existing monitoring frameworks. However, the challenges of earthquake detection and early warning remain unresolved despite recent advances and significant research efforts. Various factors contribute to this complexity, making the development and implementation of an automated P-wave detection system a highly relevant task. One of the important limitations of the existing methods is their insufficient consideration of geographical structures, surface composition, and terrain characteristics. These factors can significantly influence seismic wave propagation and detection accuracy.

Therefore, the development of neural networks tailored to specific local regions is essential to improve the reliability of earthquake early warning systems. Such region-specific models can better account for local geological variations, leading to more effective seismic monitoring and risk mitigation strategies.

In this study, we utilized convolutional neural networks for P-wave detection in the Almaty region. This region was chosen for geophysical reasons, including its high level of seismic activity. Almaty is the most seismically active zone in the Republic of Kazakhstan, situated on 27 tectonic plates. The city has experienced two devastating earthquakes in the past, making it highly likely that they will recur. Studies of this area and the regions surrounding Almaty have not been conducted sufficiently.

2. Materials and Methods

To achieve the objective of the investigation and facilitate the training of neural networks, seismic data for the Almaty region were extracted from the IRIS (Incorporated Research Institutions for Seismology) database [32–35]. The data were collected from four seismic stations within a radius of 333 km of Almaty, providing continuous and reliable seismic information. This study proposes using a convolutional neural network to detect primary waves. The key stages of our research include:

- Developing a CNN model for classification (P-wave detection) and regression (temporal parameter estimation).
- Conduct a comprehensive analysis and testing of seismic data collected from multiple stations.
- Performing a systematic evaluation of model performance, including hyperparameter tuning for optimization.
- Comparison of results with baseline models to assess the effectiveness of the proposed approach.

2.1. Dataset Collection from the IRIS

This study uses a dataset from the IRIS database. The selected geographical area is in Almaty, Kazakhstan (43.22° N, 76.92° E), with a 3.0° (~333 km) coverage radius. This

radius encompasses Almaty, the Almaty region, and parts of neighboring countries, such as Kyrgyzstan and China. The dataset consists of raw waveform data of three components sampled at 100 Hz, corresponding to the HHE, HHN, and HHZ components. Because the HHZ component allows for more efficient capture of P waves, this study uses mainly HHZ data for P-wave detection. According to IRIS data, 21 seismic stations are in the surrounding region. These stations are part of the following seismic networks: Kazakhstan (QZ) and Kyrgyzstan (KC, KN, KR). A geographic map was constructed based on coordinates, illustrating the distribution of seismic stations within a radius of 333 km from Almaty (Figure 1). The map also includes information on station elevations and operational start dates. Analysis of station elevations reveals that higher-altitude stations exhibit superior capability to record seismic events. This advantage arises from their greater distance from surface noise sources. In contrast, lowland stations are more susceptible to background noise, which may be due to human activities or meteorological conditions. As a result, high-altitude seismic stations provide cleaner recordings, notably for P waves, enhancing the reliability of seismic monitoring in the region.

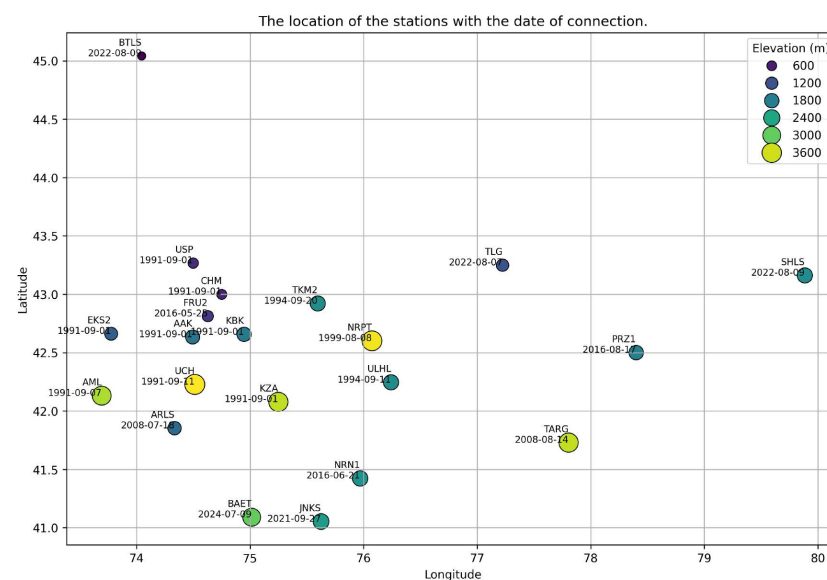


Figure 1. A geographic coordinate grid displaying the distribution of seismic stations, their elevation (represented by color intensity), and the start date of operation (labeled next to each station). The higher the station, the lighter its color, ranging from dark blue (600 m) to yellow (3600 m).

Seismic data in the IRIS database are categorized into the following accessibility classes: A, open access data; P, partially restricted access; R, restricted access; X, unavailable data—no information on availability. For this study, open-access class A data were collected from seven seismic stations (TARG, ARLS, BAET, JNKS, BTLS, SHLS, and TLG).

After analyzing the seismograms from seven stations, a slow drift was identified at some locations, such as BTLS and JNKS. To eliminate this drift and remove low-frequency noise, a 9th-order Butterworth high-pass filter with a cutoff frequency of 2 Hz was applied. This filter effectively suppressed trends and microseismic noise while preserving the key high-frequency characteristics of P waves, which is crucial for their accurate detection.

The ObsPy library retrieved and processed the seismic dataset [36]. The analysis covered two years, from 1 January 2023, to 31 December 2024. Seismic records were segmented into 240 s time windows, capturing P-wave arrivals for all available seismic events. Moreover, 219 seismic events were recorded at the seven selected stations during this period. Figure 2 illustrates the geographic distribution of these seismic stations and recorded events.

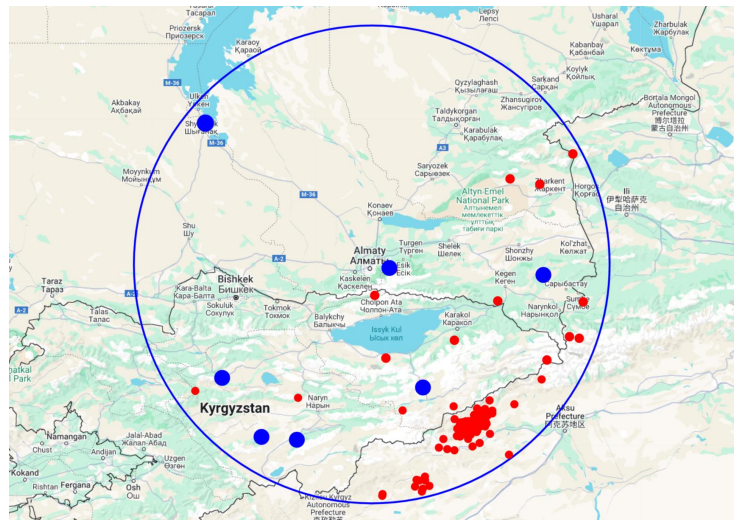


Figure 2. Fragment of the map with events. Blue dots indicate the station's coordinates on the map, and red dots are events from 1 January 2023 to 31 December 2024.

A diagram (Figure 3) was constructed to visualize the temporal distribution of seismic activity over two years. It illustrates the monthly recorded earthquakes from January 2023 to November 2024. This visualization enables the identification of periods of increased seismic activity. The highest number of seismic events was recorded in January 2024 (136 events) and February 2024 (28 events), suggesting increased tectonic activity. In contrast, the number of earthquakes in the remaining months is significantly lower, indicating the irregular nature of seismic activity in the region.

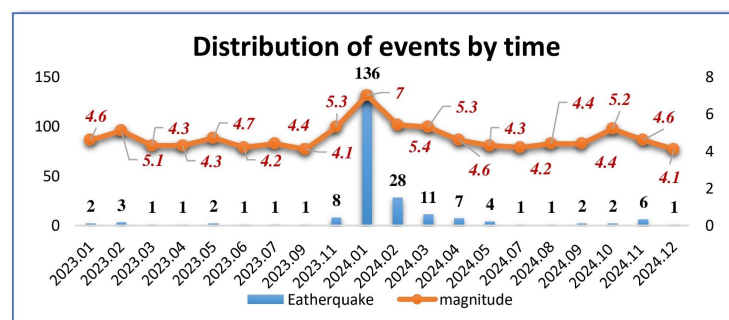


Figure 3. A diagram illustrating the monthly distribution of seismic events. The blue bars represent the number of recorded earthquakes, while the red numerical labels indicate the maximum recorded magnitudes (ranging from 4.1 to 7.0).

2.1.1. Analysis of Seismic Event Recording Quality

As part of this study, the performance of the seismic stations was evaluated to identify the characteristics of earthquake recordings in Kazakhstan and Kyrgyzstan. The analysis revealed that most of the epicenters recorded are located in Kyrgyzstan, where mountainous regions dominate the landscape. Consequently, seismic stations in remote areas of Kazakhstan, such as north of Taldykorgan or near Lake Balkhash, recorded low-intensity seismic events or, in some cases, failed to detect them.

2.1.2. Data Selection Criteria

To construct a high-quality seismic event database, the following selection criteria were applied:

1. Each recorded event included 120 s of data before and 120 s of data after the P-wave arrival.

2. To eliminate duplicate events, a minimum interval of 120 s was enforced between consecutive detections. If two seismic events were recorded within this 120-s window, one was removed from the dataset. This approach prevented multiple registrations of P waves from the same or temporally close seismic events, thereby improving the precision of seismic data analysis.

Following applying these criteria, the initial dataset of 1262 recorded events was filtered down to 1147 events, ensuring a more accurate and reliable dataset for subsequent model training and analysis. Data are presented with a minimum signal-to-noise ratio of 2 dB. Figure 4 presents a detailed statistical analysis of the quality of seismic event recordings. It illustrates the distribution of recorded events across key seismic stations for 2023–2024.

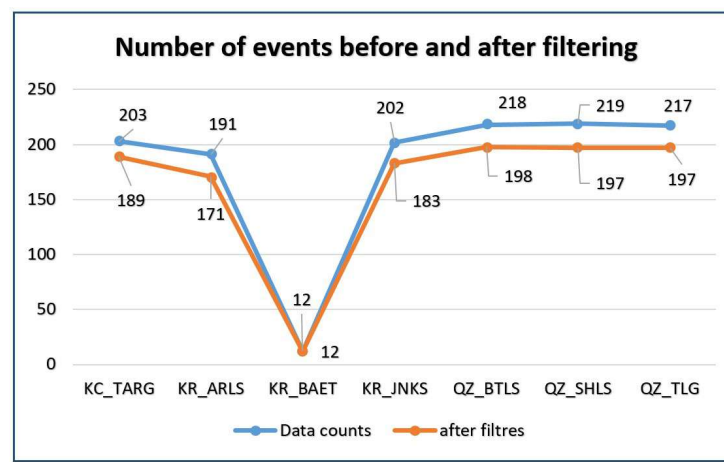


Figure 4. A diagram illustrating the number of seismic events before and after filtering.

The graph shows that most stations recorded a comparable number of seismic events. However, the BAET station detected significantly fewer events (only 12). This discrepancy is attributed to the fact that BAET was commissioned only in 2024, resulting in a much shorter observation period than the other stations.

2.2. CNN Architecture for P-Wave Detection

This study uses a convolutional neural network model to process seismic data. In contrast to traditional methods that require complex preprocessing steps, our approach allows direct analysis of raw seismic signals, uncovering hidden patterns in crustal oscillations. This capability enables the model to differentiate between longitudinal (P) and transverse (S) waves and analyze their propagation times [8]. The architecture of the proposed CNN-based approach is illustrated in Figure 5.

Seismic waveform data are recorded in three components and retrieved from the IRIS database. In the first stage of seismic data processing, the waveform information is extracted from *.mseed files using the ObsPy and pyweed libraries [37]. From the retrieved data, the signal amplitudes are extracted and subsequently processed. The time series is then segmented into fixed-length intervals, allowing the neural network to analyze each segment individually, thereby improving the detection of seismic events. The CNN model architecture used in this study is presented in Figure 6.

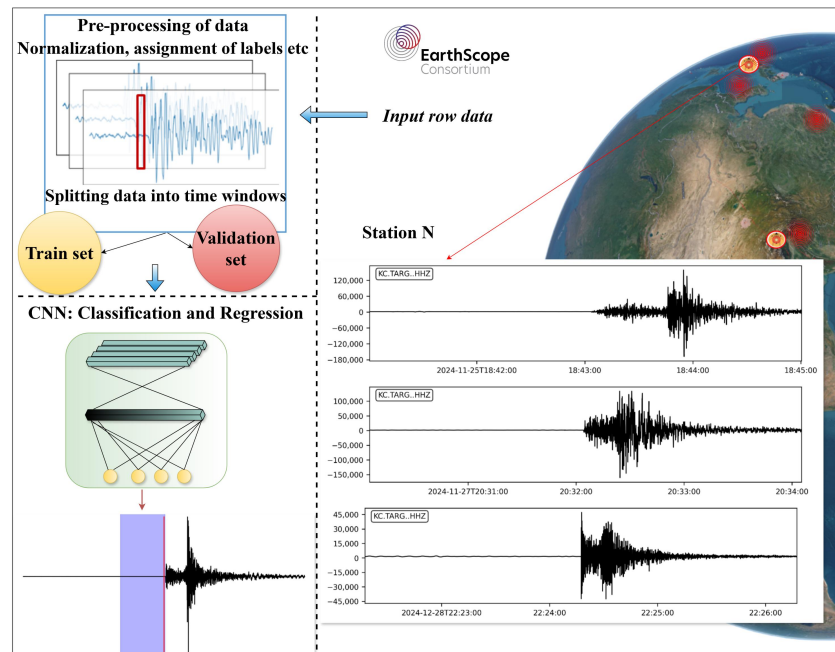


Figure 5. The data processing system structure for seismic activity detection is based on convolutional neural networks (CNNs).

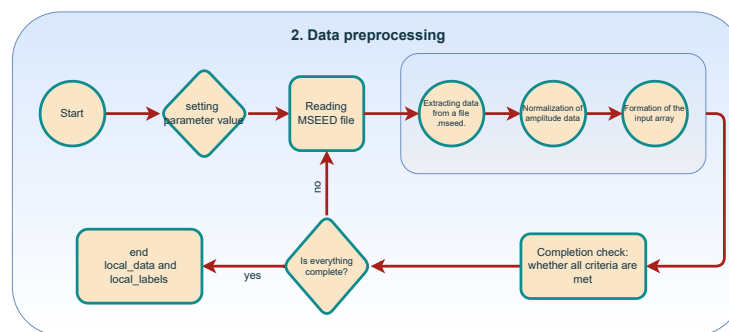


Figure 6. Block diagram of the data preprocessing algorithm.

From the extracted seismic data, the signal amplitudes are isolated and subsequently normalized to eliminate differences in scale and enhance the stability of the model. Scaling the data reduces the influence of amplitude variations, thereby improving the model performance. Normalized data are used to construct the input array for the neural network. Following preprocessing, data integrity checks are performed. The extraction and normalization process is repeated if one or more criteria are not met (e.g., missing values or invalid data entries). Once all conditions are satisfied, the data are divided into two groups: Preprocessed input data array and corresponding class labels. After completion of the preprocessing stage, the data (`local_data` and `local_labels`) undergo further analysis utilizing parallel computing techniques. A thread pool executor was implemented to optimize computational efficiency, enabling the simultaneous processing of multiple MiniSEED (*.mseed) files (Figure 7). Each file is loaded and processed in a separate thread, significantly reducing execution time.

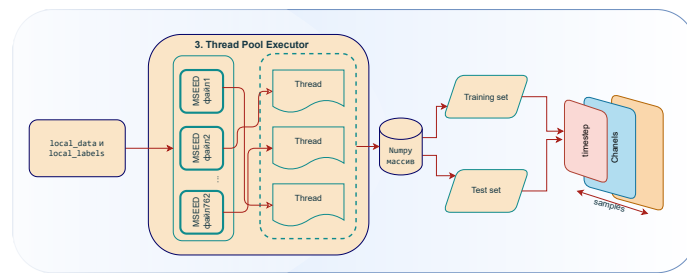


Figure 7. Implementation of the algorithm for training and validation split.

The processed data are aggregated into a unified NumPy array, which is then divided into two subsets: the training set (82%) and the validation set (18%). This ratio is a standard practice in machine learning, as it ensures a sufficient volume of data for model training while also allowing for an objective evaluation of model performance on an independent dataset.

We conducted a series of experiments, which allowed us to determine the optimal hyperparameter values for our task. This approach led to the best results in terms of P-wave detection accuracy. The structure of the proposed convolutional neural network is presented in Figure 8 and Table 1, while the model hyperparameters are listed in Table 2. The model consists of a sequence of four convolutional layers (Conv1D), each performing a one-dimensional convolution along the temporal axis of the input data. Each convolutional layer employs the ReLU activation function, effectively extracting non-linear features from seismic waveforms.

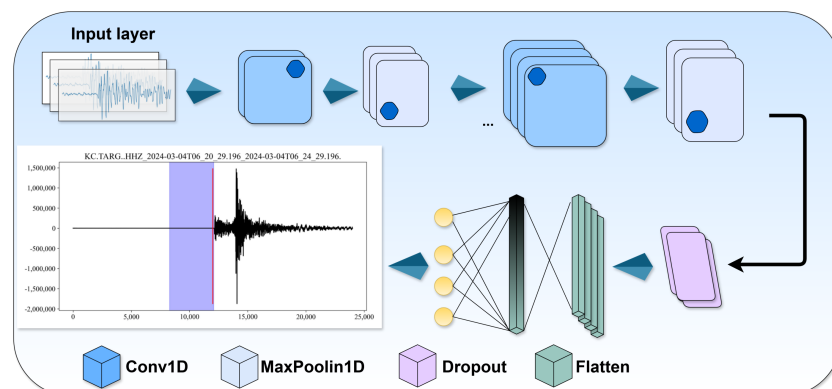


Figure 8. Convolutional neural network structure.

Each convolutional layer in the proposed model contains kernels of equal size. As a result, input features are progressively filtered, enabling the extraction of increasingly complex representations from seismic waveforms. Each convolutional layer is followed by a subsampling operation (MaxPooling1D) with a window size of 2 to reduce dimensionality and suppress noise.

Dropout layers are incorporated after the second and fourth convolutional layers to mitigate overfitting, with dropout rates of 0.5 and 0.4, respectively. This technique randomly turns off a fraction of neurons during training, preventing the model from relying too heavily on specific features and improving its generalization capabilities.

The final layer of the model consists of a fully connected dense layer. After convolution and subsampling, the output undergoes a flattening operation, which converts the multidimensional tensor into a one-dimensional vector. This representation passes through a dense layer with 16 neurons and a ReLU activation function. The final output layer consists of a single neuron with a sigmoid activation function, enabling binary classification by predicting the probability of the presence of a P-wave in the input signal.

Table 1. The architecture of the convolutional neural network includes four convolutional layers and two fully connected layers of perceptrons.

Layer	Number of Filters/ Neurons	Kernel Size	Stride	Activation Function	Additionally
Conv1D-1	32	3	1 (by default)	ReLU	input data (dim. is time- window \times fs, 1)
MaxPooling1D	16	2	2	ReLU	
Conv1D-2		3	1		
MaxPooling1D		2	2		
Dropout					Probability is 0.5
Conv1D-3	8	3	1	ReLU	Probability is 0.4
MaxPooling1D		2	2		
Conv1D-4	4	3	1	ReLU	
MaxPooling1D		2	2		
Dropout					
Flatten					Converting to 1D
Dense-1	16			ReLU	
Dense-2	1			Sigmoid	

Table 2. Hyperparameters of the model.

Parameter	Value
Optimizer	Adam
Learning rate	0.001 (default)
Loss Function	Binary Crossentropy
Metric	Accuracy
L1/L2 regularization	None
Batch size	128
Number of epochs	100

The Adam optimizer optimizes the model parameters, ensuring adaptive weight updates based on gradient descent. Since the task involves binary classification, the binary cross-entropy loss function (`databinay_crossentropy`) is used, which is well suited for two-class classification problems. The proposed CNN architecture effectively captures temporal dependencies within seismic signals while remaining adapted for binary classification. This approach improves the precision and robustness of P-wave detection by leveraging convolutional feature extraction, dimensionality reduction, and regularization techniques.

3. Results

The experiment was conducted on a high-performance computing system equipped with an NVIDIA GeForce RTX 4090 GPU, featuring 24 GB of video memory and 16,384 CUDA cores, alongside an Intel Core i9-14900K(F) processor with a clock speed of up to 6.0 GHz and 24 cores. After data filtering and preprocessing, the dataset was partitioned into training and test sets as follows:

- Training set (Train): Data from January 2023 to February 2024, comprising 935 events (82%);

- Test set (Test): Data from March 2024 to December 2024, comprising 212 events (18%).

The 82% to 18% split was selected to ensure a sufficient number of training samples while maintaining a substantial portion of data for testing, thus improving the reliability of the final evaluation results. The training set spans a complete annual cycle, allowing the model to account for seasonal variations in seismic activity. The test set was drawn from subsequent months, enabling an assessment of the model's temporal robustness and generalization ability.

The number of training epochs is a crucial factor in model optimization, as an insufficient number of epochs may lead to underfitting, whereas an excessive number can result in overfitting. An early stopping mechanism was implemented to mitigate these risks, where training continued until the validation precision stabilized. The model performed best at 300 epochs, achieving minimal validation loss while maintaining optimal generalization to unseen data. The HHZ channel data were segmented into multiple time windows to determine the optimal signal duration for P-wave detection. The time window length was systematically varied from 20 s to 40 s, with a step size of 2 s.

Figure 9 presents the relationship between the accuracy of the P-wave detection and the length of the time window. The blue dashed line represents the accuracy trend as a function of the time window size, while the blue markers indicate empirical values obtained from experiments. The red marker highlights the optimal time window length, which yields the highest detection accuracy.

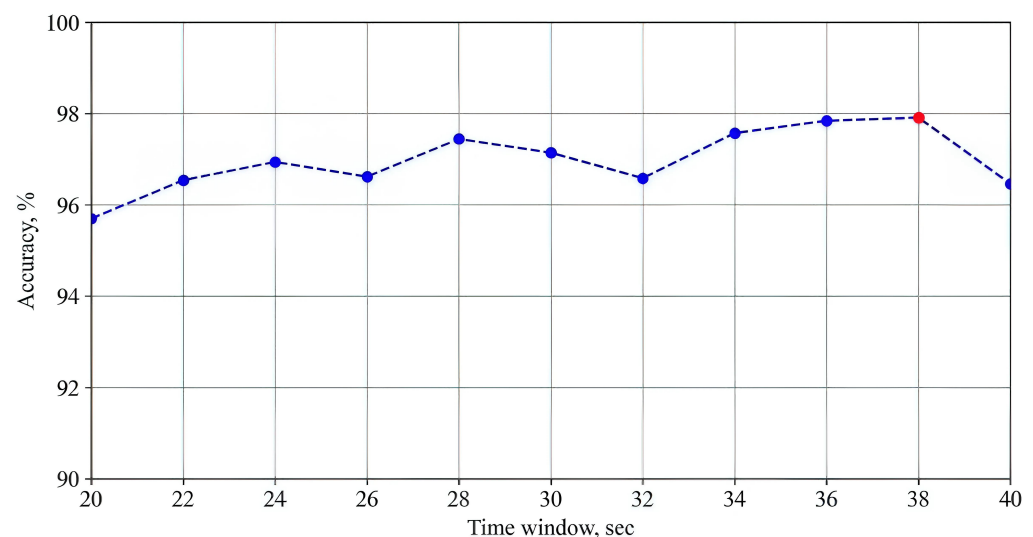


Figure 9. Optimal time window length identification. Relationship between time window length (in seconds) and classification accuracy (%).

The optimal time window length identified in this study is 38 s. This value provides the best balance between signal completeness and P-wave classification precision, allowing the model to minimize detection errors effectively. Following the selection of the optimal time window, a receiver operating characteristic (ROC) curve (Figure 10) was generated to evaluate the performance of the binary classifier. The blue curve represents the valid positive rate (sensitivity) as a function of the false positive rate, while the gray dashed line indicates the random classification baseline. The model's area under the curve (AUC) score is 0.939, indicating high precision and strong discriminative capability in detecting P waves within seismic waveforms.

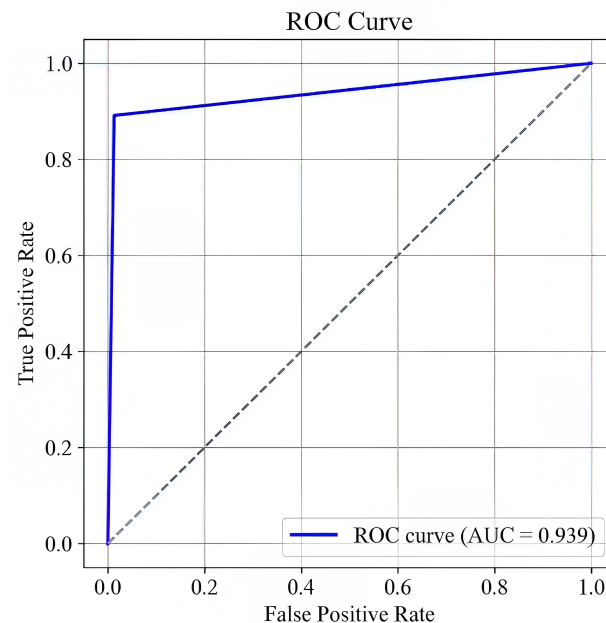


Figure 10. ROC curve of the classification model.

A confusion matrix visually represents the classification model's performance, illustrating the number of correctly and incorrectly classified instances. Figure 11 presents the confusion matrix for the model that predicts the presence or absence of P waves.

The main diagonal (0.987 and 0.891) represents the correctly classified cases:

- 98.7% of noise samples were correctly identified as noise;
- 89.1% of P-wave occurrences were accurately detected.

The off-diagonal elements indicate classification errors:

- 1.3% of noise samples were incorrectly classified as P waves (false positives);
- 10.9% of actual P waves are misclassified as noise (false negatives).

Although the model demonstrates high accuracy, a small proportion of errors remains. These misclassifications suggest areas for potential refinement, such as improving feature extraction techniques or fine-tuning decision thresholds to further enhance the performance of P-wave detection.

In addition to numerical evaluation metrics, visual analysis of results plays a crucial role in assessing model performance (Figure 12). This approach provides a qualitative understanding of how the model detects P waves within the seismic waveform over time. The key moments of signal detection are highlighted on the seismograms. This visualization allows for a direct assessment of the model's ability to pinpoint P-wave arrivals accurately, facilitating an intuitive evaluation of detection reliability and potential misclassifications.

Figure 12 presents a seismogram recorded using the HHZ channel. The blue-shaded region represents the time interval analyzed by the model, while the red line marks the exact moment when the model detected the P-wave. Before this threshold, the signal exhibits low amplitude, indicative of seismic. Following the detection point, a sharp increase in amplitude and distinct changes in waveform characteristics indicate the onset of a seismic event. This visualization method represents the model's performance, allowing for an intuitive assessment of signal behavior and the precision of P-wave arrival detection.

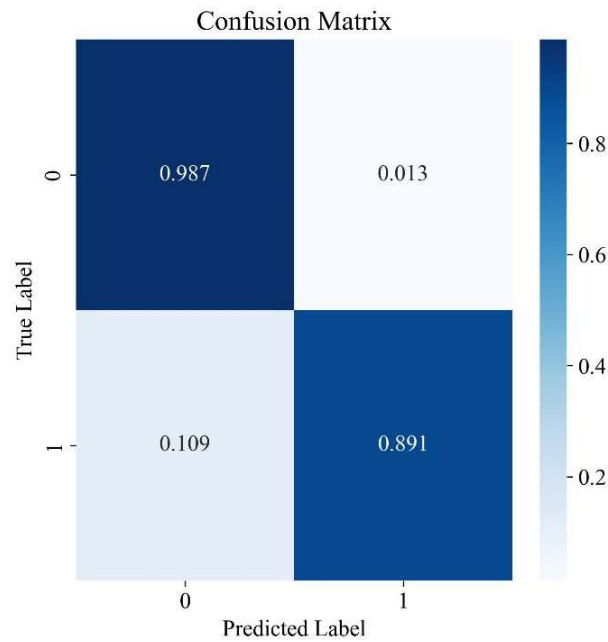


Figure 11. Error matrix for P-wave detection. 0—noise (P waves absent); 1—P waves detected.

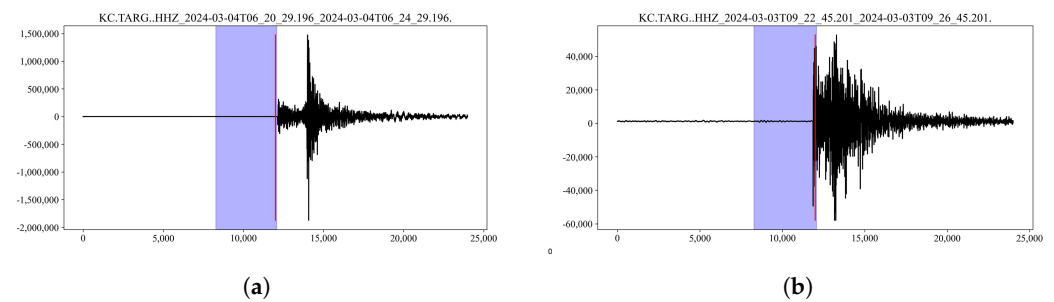


Figure 12. Seismograms with a highlighted time window and the moment of P-wave detection: (a) for the event on 4 March 2024. (b) on 3 March 2024.

Comparison

Accuracy and recall metrics were used to evaluate the effectiveness of the proposed model. These criteria provide a comprehensive assessment of the model's classification performance:

- Accuracy represents the model's ability to correctly identify P waves among all detected seismic waves, reflecting the algorithm's positive predictive value.
- Recall measures the proportion of correctly detected P waves relative to the total number of actual P waves, indicating the sensitivity of the model.

The formulas for these metrics are defined as follows:

$$accuracy = TP / (TP + FP), \quad (1)$$

$$recall = TP / (TP + FN), \quad (2)$$

here: TP (true positive): Correctly detected P waves. FP (false positive): False alarms (incorrectly detected P waves). FN (false negative): Missed detections (P waves not recognized by the model).

The performance of the proposed CNN-based model was compared to traditional and deep learning-based P-wave detection methods, including STA/LTA, PhaseNet, and GPD. The results are summarized in Table 3.

Table 3. Comparison of the proposed model with traditional P-wave detection methods.

Characteristic	STA/LTA	PhaseNet	GPD	CNN
Accuracy	0.75	0.939	0.8796	0.941
Recall	0.64	0.857	0.8038	0.891

According to Table 3, the STA/LTA method achieved the lowest recall (0.64) and accuracy (0.75), as expected as it is a classical approach that was introduced in 1978 and serves as a fundamental baseline method [4]. More advanced deep learning-based approaches were also evaluated, namely, PhaseNet, a deep neural network algorithm designed to recognize both P and S waves (recall = 0.857 and accuracy = 0.939) [23], as well as GPD, a model based on the convolutional neural network (ConvNet), which demonstrated a recall of 0.8038 and an accuracy of 0.8796 [38]. The CNN model proposed in this study achieved a recall of 0.891 and an accuracy of 0.941, outperforming the other methods regarding P-wave detection accuracy.

4. Conclusions

This study developed and trained a convolutional neural network for the automatic detection of P waves in seismic data. Experimental results demonstrated that the proposed method achieved a P-wave detection accuracy of 94.1% and a recall of 89.1%, making it comparable to some of the best deep learning-based approaches currently available.

The model used seismic data from the IRIS database for training and testing, collected from seven seismic stations within a 333 km radius of Almaty. The Almaty region is one of the most seismically active areas in the country, making the dataset highly unique and valuable for this region. The complex terrain and diverse geological characteristics introduce additional challenges for seismic wave detection, further emphasizing the significance of the proposed approach.

One of the key advantages of the developed model is its high accuracy and reliability in P-wave detection, which is critical for precise and timely seismic activity analysis. Using convolutional neural networks enables the automation of large-scale seismic data analysis, eliminating the need for manual annotation of specific regions and significantly accelerating the detection process. This is one of the developed model's key advantages.

Furthermore, the method has shown a high degree of adaptability to local geophysical characteristics, allowing for effective monitoring of seismic activity in complex and geologically diverse regions.

Author Contributions: Conceptualization, D.Z., A.A. (Aldiyar Agishev) and A.S.; methodology, M.I.; software, D.Z., G.K. and A.O.; validation, G.K., A.O. and A.A. (Almansur Agishev); formal analysis, S.K.; investigation, D.Z. and A.S.; resources, M.I. and A.A. (Aldiyar Agishev); data curation, G.K. and A.A. (Almansur Agishev); writing—original draft preparation, A.S.; writing—review and editing, A.A. (Aldiyar Agishev) and A.A. (Almansur Agishev); visualization, A.S.; supervision, M.I. and S.K.; project administration, S.K.; funding acquisition, M.I. and A.A. (Aldiyar Agishev). All authors have read and agreed to the published version of the manuscript.

Funding: This research was funded by the Science Committee of the Ministry of Science and Higher Education of the Republic of Kazakhstan (grant no. AP23488521).

Institutional Review Board Statement: Not applicable.

Informed Consent Statement: Not applicable.

Data Availability Statement: All seismic data were downloaded through the EarthScope Consortium Web Services accessed on 15 January 2025 (https://www.iris.edu/app/station_monitor/). All data collected in this study can be provided directly by the corresponding author upon reasonable request.

Acknowledgments: I.M. thanks the Science Committee of the Ministry of Science and Higher Education of the Republic of Kazakhstan (grant no. AP23488521) for its support of that study. The facilities of EarthScope Consortium were used for access to waveforms, related metadata, and/or derived products used in this study. These services are funded through the National Science Foundation's Seismological Facility for the Advancement of Geoscience (SAGE) Award under Cooperative Agreement EAR-1724509.

Conflicts of Interest: The authors declare that there are no conflicts of interest regarding the publication of this article.

References

1. Basher, R.E. Global early warning systems for natural hazards: Systematic and people-centred. *Philos. Trans. R. Soc. A Math. Phys. Eng. Sci.* **2006**, *364*, 2167–2182. [\[CrossRef\]](#)
2. Cremen, G.; Galasso, C. Earthquake early warning: Recent advances and perspectives. *Earth-Sci. Rev.* **2020**, *205*, 103184. [\[CrossRef\]](#)
3. Ross, Z.E.; Meier, M.A.; Hauksson, E. P Wave Arrival Picking and First-Motion Polarity Determination with Deep Learning. *J. Geophys. Res. Solid Earth* **2018**, *123*, 5120–5129. [\[CrossRef\]](#)
4. Allen, R.V. Automatic earthquake recognition and timing from single traces. *Bull. Seismol. Soc. Am.* **1978**, *68*, 1521–1532. [\[CrossRef\]](#)
5. Leonard, M.; Kennett, B. Multi-component autoregressive techniques for the analysis of seismograms. *Phys. Earth Planet. Inter.* **1999**, *113*, 247–263. [\[CrossRef\]](#)
6. Zhu, W.; Li, X.; Liu, C.; Xue, F.; Han, Y. An STFT-LSTM System for P-Wave Identification. *IEEE Geosci. Remote. Sens. Lett.* **2020**, *17*, 519–523. [\[CrossRef\]](#)
7. Mousavi, S.M.; Beroza, G.C. A Machine-Learning Approach for Earthquake Magnitude Estimation. *Geophys. Res. Lett.* **2020**, *47*, e2019GL085976. [\[CrossRef\]](#)
8. Bilal, M.A.; Ji, Y.; Wang, Y.; Akhter, M.P.; Yaqub, M. Early Earthquake Detection Using Batch Normalization Graph Convolutional Neural Network (BNGCNN). *Appl. Sci.* **2022**, *12*, 7548. [\[CrossRef\]](#)
9. Li, Z.; Meier, M.A.; Hauksson, E.; Zhan, Z.; Andrews, J. Machine Learning Seismic Wave Discrimination: Application to Earthquake Early Warning. *Geophys. Res. Lett.* **2018**, *45*, 4773–4779. [\[CrossRef\]](#)
10. Chandrakumar, C.; Prasanna, R.; Stephens, M.; Tan, M.L.; Holden, C.; Punchihewa, A.; Becker, J.S.; Jeong, S.; Ravishan, D. Algorithms for detecting P-waves and earthquake magnitude estimation: Initial literature review findings. In Proceedings of the ISCRAM Asia Pacific Conference, Melbourne, Australia, 7–9 November 2022; pp. 138–155.
11. Meier, M.A.; Ross, Z.E.; Ramachandran, A.; Balakrishna, A.; Nair, S.; Kundzicz, P.; Li, Z.; Andrews, J.; Hauksson, E.; Yue, Y. Reliable Real-Time Seismic Signal/Noise Discrimination With Machine Learning. *J. Geophys. Res. Solid Earth* **2019**, *124*, 788–800. [\[CrossRef\]](#)
12. Trani, L.; Pagani, G.A.; Zanetti, J.P.P.; Chapeland, C.; Evers, L. DeepQuake—An application of CNN for seismo-acoustic event classification in The Netherlands. *Comput. Geosci.* **2022**, *159*, 104980. [\[CrossRef\]](#)
13. Yoon, C.E.; O'Reilly, O.; Bergen, K.J.; Beroza, G.C. Earthquake detection through computationally efficient similarity search. *Sci. Adv.* **2015**, *1*, e1501057. [\[CrossRef\]](#)
14. Xu, S.; Zhang, C.; Chen, Z.; Li, Y.; Liu, J. Accurate identification of microseismic waveforms based on an improved neural network model. *J. Appl. Geophys.* **2021**, *190*, 104343. [\[CrossRef\]](#)
15. Chen, Y. Automatic microseismic event picking via unsupervised machine learning. *Geophys. J. Int.* **2020**, *222*, 1750–1764. [\[CrossRef\]](#)
16. Chen, Y. Fast waveform detection for microseismic imaging using unsupervised machine learning. *Geophys. J. Int.* **2018**, *215*, 1185–1199. [\[CrossRef\]](#)
17. Indi, M.W.P.; Novianty, A.; Prasasti, A.L. Automatic First Arrival Picking on P-Wave Seismic Signal Using Support Vector Machine Method. In Proceedings of the 2020 8th International Conference on Information and Communication Technology (ICoICT), Yogyakarta, Indonesia, 24–26 June 2020; pp. 1–6. [\[CrossRef\]](#)
18. Hafez, A.G.; Rabie, M.; Kohda, T. Seismic noise study for accurate P-wave arrival detection via MODWT. *Comput. Geosci.* **2013**, *54*, 148–159. [\[CrossRef\]](#)
19. Li, Z.; Peng, Z.; Hollis, D.; Zhu, L.; McClellan, J. High-resolution seismic event detection using local similarity for Large-N arrays. *Sci. Rep.* **2018**, *8*, 1646. [\[CrossRef\]](#)
20. Yasaka, K.; Hatano, S.; Mizuki, M.; Okimoto, N.; Kubo, T.; Shibata, E.; Watadani, T.; Abe, O. Effects of deep learning on radiologists' and radiology residents' performance in identifying esophageal cancer on CT. *Br. J. Radiol.* **2023**, *96*, 20220685. [\[CrossRef\]](#)

21. Fang, W.; Chen, Y.; Xue, Q. Survey on Research of RNN-Based Spatio-Temporal Sequence Prediction Algorithms. *J. Big Data* **2021**, *3*, 97–110. [CrossRef]
22. Saad, O.M.; Chen, Y. Earthquake Detection and P-Wave Arrival Time Picking Using Capsule Neural Network. *IEEE Trans. Geosci. Remote. Sens.* **2021**, *59*, 6234–6243. [CrossRef]
23. Zhu, W.; Beroza, G.C. PhaseNet: A deep-neural-network-based seismic arrival-time picking method. *Geophys. J. Int.* **2018**, *216*, 261–273. [CrossRef]
24. Holmstrom, L.; Christensen, M.; Yuan, N.; Hughes, J.W.; Theurer, J.; Jujjavarapu, M.; Fatehi, P.; Kwan, A.; Sandhu, R.K.; Ebinger, J.; et al. Deep learning-based electrocardiographic screening for chronic kidney disease. *Commun. Med.* **2023**, *3*, 73. [CrossRef] [PubMed]
25. Chamarty Anusha, P.S.A. Object Detection using Deep Learning. *Int. J. Comput. Appl.* **2018**, *182*, 18–22. [CrossRef]
26. Huang, L.; Li, J.; Hao, H.; Li, X. Micro-seismic event detection and location in underground mines by using Convolutional Neural Networks (CNN) and deep learning. *Tunn. Undergr. Space Technol.* **2018**, *81*, 265–276. [CrossRef]
27. Wang, Y.; Li, X.; Wang, Z.; Shi, J.; Bao, E. Deep learning for P-wave arrival picking in earthquake early warning. *Earthq. Eng. Eng. Vib.* **2021**, *20*, 391–402. [CrossRef]
28. Wei, W.; Huerta, E.A.; Whitmore, B.C.; Lee, J.C.; Hannon, S.; Chandar, R.; Dale, D.A.; Larson, K.L.; Thilker, D.A.; Ubeda, L.; et al. Deep transfer learning for star cluster classification: I. application to the PHANGS–HST survey. *Mon. Not. R. Astron. Soc.* **2020**, *493*, 3178–3193. [CrossRef]
29. Shickel, B.; Tighe, P.J.; Bihorac, A.; Rashidi, P. Deep EHR: A Survey of Recent Advances in Deep Learning Techniques for Electronic Health Record (EHR) Analysis. *IEEE J. Biomed. Health Inform.* **2018**, *22*, 1589–1604. [CrossRef]
30. Hsu, T.Y.; Huang, C.W. Onsite Early Prediction of PGA Using CNN with Multi-Scale and Multi-Domain P-Waves as Input. *Front. Earth Sci.* **2021**, *9*, 626908. [CrossRef]
31. Chandrakumar, C.; Tan, M.L.; Holden, C.; Stephens, M.; Punchihewa, A.; Prasanna, R. Estimating S-wave amplitude for earthquake early warning in New Zealand: Leveraging the first 3 s of P-Wave. *Earth Sci. Inform.* **2024**, *17*, 4527–4554. [CrossRef]
32. LTD Seismological Experience and Methodology Expedition of the Committee of Science of the Ministry of Education and Science of the Republic of Kazakhstan. Seismic Network of the Seismological Experience and Methodology Expedition CS MES RK. 2003. Available online: <https://www.fdsn.org/networks/detail/QZ/> (accessed on 15 January 2025). [CrossRef]
33. Central Asian Institute for Applied Geosciences. Central Asian Seismic Network of CAIAG. 2008. Available online: <https://www.fdsn.org/networks/detail/KC/> (accessed on 15 January 2025). [CrossRef]
34. Kyrgyz Institute of Seismology, IVTAN/KIS; University of California, San Diego. Kyrgyz Seismic Telemetry Network. 1991. Available online: <https://www.fdsn.org/networks/detail/KN/> (accessed on 15 January 2025). [CrossRef]
35. Kyrgyz Institute of Seismology, KIS. Kyrgyz Digital Network. 2007. Available online: <https://www.fdsn.org/networks/detail/KR/> (accessed on 15 January 2025). [CrossRef]
36. The ObsPy Development Team. Obspy 1.4.1. 2024. Available online: <https://zenodo.org/records/11093256> (accessed on 18 November 2024). [CrossRef]
37. Falco, N.; Clark, A.; Trabant, C. Wilber and pyweed: Event-based seismic data request tools. In Proceedings of the AGU Fall Meeting Abstracts, New Orleans, LA, USA, 11–15 December 2017; Volume 2017, p. T44D-06.
38. Ross, Z.E.; Meier, M.; Hauksson, E.; Heaton, T.H. Generalized Seismic Phase Detection with Deep Learning. *Bull. Seismol. Soc. Am.* **2018**, *108*, 2894–2901. [CrossRef]

Disclaimer/Publisher’s Note: The statements, opinions and data contained in all publications are solely those of the individual author(s) and contributor(s) and not of MDPI and/or the editor(s). MDPI and/or the editor(s) disclaim responsibility for any injury to people or property resulting from any ideas, methods, instructions or products referred to in the content.